Visual Neuroscience (2009), **26**, 329–340. Printed in the USA.

doi:10.1017/S0952523809990083

Improved visual sensitivity during smooth pursuit eye movements: Temporal and spatial characteristics

ALEXANDER C. SCHÜTZ, DORIS I. BRAUN, AND KARL R. GEGENFURTNER

Abteilung Allgemeine Psychologie, Justus-Liebig-Universität, Giessen, Germany

(RECEIVED December 17, 2008; ACCEPTED May 31, 2009; FIRST PUBLISHED ONLINE July 15, 2009)

Abstract

Recently, we showed that contrast sensitivity for color and high–spatial frequency luminance stimuli is enhanced during smooth pursuit eye movements (Schütz et al., 2008). In this study, we investigated the enhancement over a wide range of temporal and spatial frequencies. In Experiment 1, we measured the temporal impulse response function (TIRF) for colored stimuli. The TIRF for pursuit and fixation differed mostly with respect to the gain but not with respect to the natural temporal frequency. Hence, the sensitivity enhancement seems to be rather independent of the temporal frequency of the stimuli. In Experiment 2, we measured the spatial contrast sensitivity function for luminance-defined Gabor patches with spatial frequencies ranging from 0.2 to 7 cpd. We found a sensitivity improvement during pursuit for spatial frequencies above 2–3 cpd. Between 0.5 and 3 cpd, sensitivity was impaired by smooth pursuit eye movements, but no consistent difference was observed below 0.5 cpd. The results of both experiments are consistent with an increased contrast gain of the parvocellular retinogeniculate pathway.

Keywords: Smooth pursuit eye movements, Temporal contrast sensitivity, Temporal Impulse Response, Spatial contrast sensitivity, Color contrast sensitivity, Sensitivity enhancement

Introduction

Primates use saccadic eye movements to shift their gaze to interesting objects. By doing this, the object is projected on the fovea, the part of the retina with the highest visual acuity. If the inspected object is moving, it can be stabilized on the retina by means of smooth pursuit eye movements. This essentially prevents blurring by retinal motion. Both the maximization of visual acuity and the minimization of retinal motion are clearly beneficial for the recognition of the tracked object.

Besides these retinal consequences of saccades and smooth pursuit, there are also nonretinal influences on visual perception. Since the early work of Holt (1903), it is known that saccades affect visual sensitivity. More recently, it has been shown that luminance sensitivity for low spatial frequencies is selectively suppressed, while color sensitivity and luminance sensitivity for high spatial frequencies are unaffected (Burr et al., 1994). It is also known that the suppression is caused actively by an efference copy or corollary discharge (Sperry, 1950; von Holst & Mittelstaedt, 1950; Diamond et al., 2000; Wurtz, 2008). Recently, we showed that not only saccadic but also smooth pursuit eye movements affect visual sensitivity: during smooth pursuit, the sensitivity for colored stimuli and luminance stimuli containing high spatial frequencies is enhanced (Schütz et al., 2008). This enhancement precedes the onset of smooth pursuit by approximately 50 ms and scales positively with smooth pursuit velocity.

Address correspondence and reprint requests to: Abteilung Allgemeine Psychologie, Justus-Liebig-Universität, Otto-Behaghel-Str. 10F, 35394 Giessen, Germany. E-mail: alexander.c.schuetz@psychol.uni-giessen.de

One can imagine several ways to accomplish such an enhancement of contrast sensitivity. First, it might be that the amount of temporal (Watson, 1986) or spatial (Olzak & Thomas, 1986) summation is increased. For instance, it has been shown that the amount of temporal and spatial summation is modulated by the intensity of the background (Barlow, 1958). Increasing the temporal or spatial summation leads to an improvement of sensitivity at lower temporal and spatial frequencies but also to a reduction of sensitivity at higher temporal and spatial frequencies. Hence, an increase of summation is not very probable because we previously found an improvement of sensitivity during pursuit for red–green flicker of high temporal frequency as well as for high–spatial frequency luminance stimuli. On the other hand, the spatial and temporal summation might be decreased. This would result in an improvement at high temporal and spatial frequencies but also in an impairment at low temporal and spatial frequencies. This hypothesis would be consistent with our findings of an enhancement at high temporal and spatial frequencies. Both the decrease and the increase of summation would change the contrast sensitivity function mainly at the extreme ends of the visible frequency axis. However, the integral of the contrast sensitivity function would not change, which means that the overall sensitivity is not changed. Finally, a general increase in sensitivity might also be accomplished by an increased contrast gain of a neural subpopulation. For instance, recent experiments show that attention can modulate neural activity as early as in the lateral geniculate nucleus (LGN) (O'Connor et al., 2002; McAlonan et al., 2008). In the present study, we investigated the temporal and spatial characteristics of the sensitivity enhancement during smooth pursuit. By doing so, we strived to gain insight into the underlying mechanism of the enhancement.

Experiment 1: Temporal impulse response functions for color

Since we found an improvement for red–green flicker at 16 Hz as well as for briefly flashed stimuli, we argued that the sensitivity improvement is not accomplished by an increased temporal summation (Schütz et al., 2008). In sharp contrast to temporal summation, it has been suggested that the chromatic temporal resolution is increased during smooth pursuit (Terao et al., 2008). An increase of temporal resolution, however, might be a result of two different mechanisms: First, it might be that the temporal impulse response function (TIRF) becomes faster, which would mean that sensitivity is improved only for high temporal frequencies. Second, it might be that the overall contrast sensitivity is increased, which would among other things increase the temporal resolution. In Experiment 1, we wanted to clarify whether the enhancement of chromatic contrast sensitivity during pursuit is indeed caused by a shift of the TIRF or if there is an overall increase of chromatic sensitivity. To this end, we compared TIRF for color during fixation and smooth pursuit.

A lot of studies investigated TIRF, both psychophysically and physiologically, and several differences between the TIRF for color and luminance have been observed. Psychophysically, it has been shown that the TIRF for luminance is biphasic with a strong suppression (Ikeda, 1965; Rashbass, 1970), whereas the TIRF for color is monophasic (Uchikawa & Ikeda, 1986; Burr & Morrone, 1993) or only slightly biphasic (Eskew et al., 1994). Physiology showed that the TIRF of "color-blind" magnocellular neurons speeds up with increasing stimulus contrast, whereas color-opponent parvocellular neurons do not change their impulse response (Lee et al., 1994; Benardete & Kaplan, 1999).

For luminance processing, there is some evidence that the TIRF shows a higher natural temporal frequency during smooth pursuit (Bedell et al., 2003; Tong et al., 2006). Consistent with that finding, we observed a trend for a shift of the temporal contrast sensitivity function (TCSF) for luminance to higher temporal frequencies during smooth pursuit and a significant reduction of the sensitivity at all temporal frequencies (Schütz et al., 2007). During saccades, the TIRF is also accelerated for luminance but not for color (Burr & Morrone, 1996).

Materials and methods

Design

We estimated TIRF by measuring contrast sensitivity for pairs of stimuli that were successively presented. Stimulus pairs have been used for a long time to estimate the temporal properties of the visual system during fixation (Ikeda, 1965; Rashbass, 1970; Burr & Morrone, 1993) and have also been applied during eye movements (Burr & Morrone, 1996; Bedell et al., 2008). We tested 10 different stimulus onset asynchronies (SOAs) between stimulus pairs: 0, 10, 20, 30, 40, 60, 80, 120, 150, and 200 ms. The stimulus pair was either in phase (IN), meaning that both stimuli had the same contrast modulation, or out of phase (OUT), meaning that they had opposite contrast modulations. Each condition (SOA plus contrast modulation) was tested during fixation and smooth pursuit. This resulted in a 10 (SOA) $\times$ 2 (contrast modulation) $\times$ 2 (eye movement condition) design matrix. Subjects performed the experiment in several sessions; in each session, one SOA was tested in all other conditions.

Subjects

One of the authors (A.C.S.) and one naïve subject (HO) participated in the experiments. The naïve subject was a male student of the Justus-Liebig-University who was paid for his participation. Both subjects had normal or corrected to normal vision.

Equipment

Subjects were seated in a dimly lit room facing a 21-inch CRT monitor (ELO Touchsystems, Fremont, CA) driven by a Nvidea Quadro NVS 285 graphics board with a refresh rate of 100 Hz noninterlaced. The gamma nonlinearity of the monitor was measured with a Laser 2000 Model 370 Photometer (UDT Instruments, Baltimore, MD) and corrected using a lookup table. At a viewing distance of 47 cm, the active screen area subtended 45 deg in the horizontal direction and 36 deg vertical on the subject's retina. With a spatial resolution of 1280 $\times$ 1024 pixels, this results in 28 pixels/deg. The subject's head was fixed in place using a chin rest.

Eye movement recording and analysis

Eye position signals were recorded with a head-mounted video-based eye tracker (EyeLink II; SR Research Ltd., Osgoode, Ontario, Canada) and were sampled at 250 Hz. Subjects viewed the display binocularly. Stimulus display and data collection were controlled by a PC. We obtained eye velocity signals by digital differentiation of eye position signals over time. The eye position and velocity signals were filtered by a Butterworth filter with cutoff frequencies of 30 and 20 Hz, respectively. To determine smooth pursuit gain, we divided the eye velocity by the pursuit target velocity in a 150-ms interval, 1250 ms after pursuit target motion onset. To detect saccades, we used a cutoff criterion (75,000 deg/s^3) on the third derivative of eye position (Wyatt, 1998). Trials containing saccades in an interval of 100 ms centered on stimulus presentation (7% for subject A.C.S. and 4% for HO), and trials with a pursuit gain lower than 0.7 (1% for both subjects) were discarded and then repeated.

Visual stimuli

We used a black bull's-eye with an outer radius of 0.3 deg and an inner radius of 0.15 deg as pursuit respective fixation target. To measure contrast sensitivity, we used horizontal lines. The lines spanned the whole screen width and were vertically modulated by a Gaussian distribution with an s.d. of 0.15 deg. Each line was flashed for one refresh cycle of the monitor. At a refresh rate of 100 Hz, this gives a nominal stimulus duration of 10 ms. Due to the decay of phosphors, the actual stimulus duration was shorter. Using a stimulus that was parallel to stimulus motion and by flashing it just for a brief period of time, we wanted to make sure that no retinal image motion was induced by the eye movements. The lines were modulated in contrast along the L–M axis of the DKL color space (Derrington et al., 1984). The same stimuli have been used in our previous studies on chromatic contrast sensitivity (Schütz et al., 2008, 2009). The contrast type of the first line was determined randomly (L or M). The contrast of the second line resulted from the contrast of the first line and the phase condition.

Experimental procedure

At the beginning of each trial, a black bull's-eye with an outer radius of 0.3 deg and an inner radius of 0.075 deg appeared at the screen center. The subjects had to fixate the bull's-eye and press an assigned button to start the trial. This triggered the EyeLink II System to perform a drift correction to correct errors of headband slippage or other factors. If the drift correction succeeded, the initial bull's-eye disappeared and was replaced by the eye movement

target. In fixation trials, we presented the bull's-eye for 1500 ms at the center of the screen, where observers had to keep fixation. One thousand milliseconds after the beginning of the trial, we flashed the first stimulus for 10 ms, 2 deg above or below the bull's-eye. The second stimulus was flashed at the respective SOA. In pursuit trials, we presented the bull's-eye at 13 deg left or right of the center of the screen. After 250 ms, the bull's-eye moved toward the screen center at a velocity of 10.6 deg/s, and observers were instructed to track it as accurately as possible. When the bull's-eye reached the screen center, we flashed the first stimulus and the second stimulus with the respective SOA. Motion continued for another 500 ms. Subjects had to indicate if the pair of lines appeared above or below the bull's-eye at the end of the trial.

Psychophysical data analysis

We adjusted the contrast of the stimulus pair according to a staircase procedure (Levitt, 1971) and obtained thresholds by fitting the percentage of correct answers for the different contrast levels with a cumulative Gaussian function. We used the Psignifit toolbox in Matlab to fit the psychometric function (Wichmann & Hill, 2001). Different functions have been used previously to fit TIRF (Burr & Morrone, 1993; Bedell et al., 2008). We fitted both functions to our data and finally chose the function used by Bedell et al., 2008 because it provided a similar quality of fits with a smaller number of free parameters. This function describes a second-order linear system by three free parameters: the response amplitude, A; the natural temporal frequency, W (in radians/s); and the damping ratio, D. For convenience, all values of the natural temporal frequency W are given in Hertz.

$$\begin{aligned} 0 \le D < 1 : R(t) &= (A \times W/\sqrt{1-D^2}) \times \exp \\ &\quad (-D \times W \times t) \times \sin(W \times \sqrt{1-D^2} \times t) \\ D = 1 : R(t) &= (A \times W^2) \times \exp(-D \times W \times t) \times t \\ D \ge 1 : R(t) &= (A \times W/2 \times \sqrt{D^2-1}) \times \exp \\ &\quad [-(D-\sqrt{D^2-1}) \times W \times t] - (A \times W/2 \times \sqrt{D^2-1}) \\ &\quad \times \exp[-(D+\sqrt{D^2-1}) \times W \times t. \end{aligned} \tag{1}$$

The response for a pair of stimuli is given by eqn. (2). The sign depends on the phase condition. The responses are subtracted for out-of-phase stimuli and added for in-phase stimuli.

$$R(t, \mathrm{SOA}) = R(t) \pm R(t - \mathrm{SOA}). \tag{2}$$

Finally, the contrast sensitivity is obtained by summing the responses (Watson, 1979) in 1000-ms interval (eqn. 3).

$$\mathrm{CS}(\mathrm{SOA}) = \left[\sum_{t=0}^{1000} |R(t, \mathrm{SOA})|^{3.5} \right]^{1/3.5}. \tag{3}$$

We determined the three free parameters by means of minimization of the sum of the squared errors (RSS).

To figure out how the impulse response functions differ between fixation and pursuit, we fitted different types of models and compared their ability to explain the data. These models could not be compared solely on the basis of the RSS because they differed in respect to the number of free parameters. Hence, we calculated the Akaike information criterion (AIC) (Akaike, 1974) according to eqn. (4) and the Bayesian information criterion (BIC) (Schwarz, 1978) according to eqn. (5) to compare the quality of the different models. n gives the number of fitted data points; k, the number of free parameters in the model (plus one to include the residual sum of squares, which also belongs to the estimated parameters); and RSS, the residual sum of squares.

$$\mathrm{AIC}_c = n \times \ln(\mathrm{RSS}/n) + 2k + 2k(k+1)/n - k - 1. \tag{4}$$

$$\mathrm{BIC} = n \times \ln(\mathrm{RSS}\ n) + k \times \ln(n). \tag{5}$$

We calculated for both indices the difference between the individual values and the lowest value according to eqn. (6) (Burnham & Anderson, 2002) because absolute values of AIC and BIC are not meaningful.

$$\Delta \mathrm{IC}_i = \mathrm{IC}_i - \mathrm{IC}_{\min}. \tag{6}$$

Finally, we calculated the relative weights for each model as in eqn. (7) (Burnham & Anderson, 2002). This probability estimates which model is most likely the ''true'' model.

$$p_i = \mathrm{e}^{-0.5\Delta \mathrm{IC}_i} \Big/ \sum_{r=1}^{R} \mathrm{e}^{-0.5\Delta \mathrm{IC}_r}. \tag{7}$$

We tested eight different models: In the two extreme models, either all parameters were allowed to be different between fixation and pursuit (none) or all parameters had to be identical for fixation and pursuit (A&W&D). In the intermediate models, either one (A, W, or D) or two (A&W, A&D, or W&D) of the parameters had to be identical for fixation and pursuit. Each model is named after the parameters that are fixed to equal values during fixation and pursuit.

Results

Here, we measured chromatic sensitivity for two-pulse stimuli at 2-deg eccentricity. As we were primarily interested in sensitivity differences between fixation and pursuit, we first analyzed the sensitivity ratios between fixation and pursuit (Fig. 1). Sensitivity during pursuit was higher than during fixation for all experimental conditions. This result by itself is not compatible with the assumption of a shift of the TIRF for color during smooth pursuit. In this case, sensitivities during pursuit should only be higher for some SOAs but also lower for other SOAs. On average, the sensitivity ratio amounted to 1.24 (s.d. 0.14) for subject A.C.S. and 1.23 (s.d. 0.13) for subject HO. The maximum sensitivity ratio of 1.57 was reached at SOAs of 40 (A.C.S.) respective 30 (HO) ms.

To do a more thorough analysis, we fitted different TIRFs to the data. The models differed in respect to the constraints on parameter differences between fixation and pursuit. Fig. 2 shows the root mean square error (RMSE) and the relative probability of AIC and BIC for all models. All models provided a good fit to the data, indicated by the small RMSE, except for the model that did not allow any differences between fixation and pursuit (A&W&D).

As the models differed in the number of free parameters, we determined the best model on the basis of the AIC and BIC (Fig. 2). For both subjects, the relative probability of the AIC and BIC was highest for the model with a fixed temporal frequency and a fixed damping ratio (W&D). For this model, the relative probability of the AIC reached 0.53 for subject A.C.S. and 0.43 for subject HO. The relative probability of the BIC reached even higher values, 0.61 and 0.53 for A.C.S. and HO, respectively. Hence, the W&D model accounted best for the data. This indicates that the differences

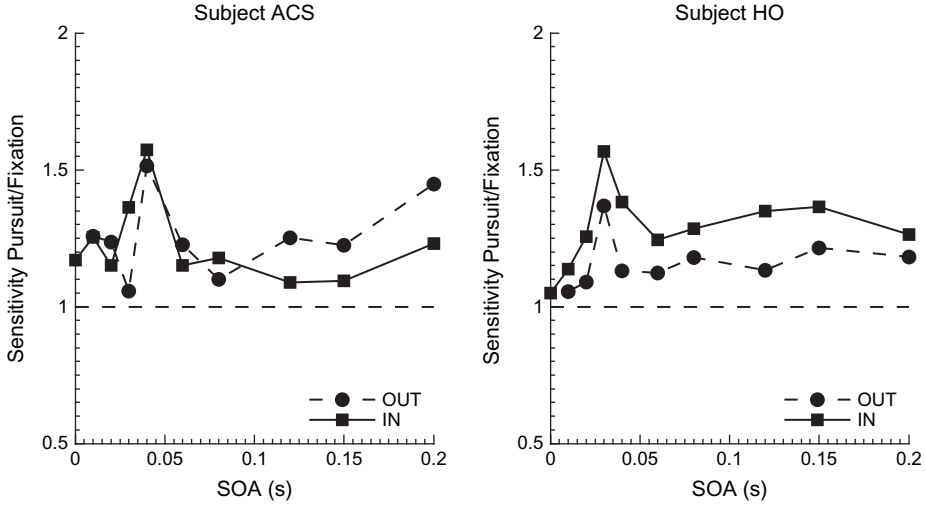

Fig. 1. Experiment 1: Color sensitivity ratio between fixation and pursuit. The dotted lines and circles represent out-of-phase stimulation, and the continuous line and squares represent in-phase stimulation. Markers represent measured sensitivity ratios; the lines are obtained by linear interpolation. The dashed horizontal line indicates points with equal sensitivity during fixation and pursuit.

between pursuit and fixation were mostly governed by different response amplitudes. The comparison between the models with one fixed parameter (A, W, or D) pointed in the same direction: As all these models had the same number of free parameters, the AIC and BIC depended solely on the RSS. The relative probability for the model with a fixed response amplitude (*A*) was lower by at least 0.1 for the AIC and 0.07 for the BIC when compared to the models with a fixed temporal frequency (*W*) or with a fixed damping ratio (*D*). This also indicates that different response amplitudes were the major source of the sensitivity differences between pursuit and fixation.

In the next step, we compared the fitted parameter values during pursuit and fixation (Fig. 3; **Supplemental Table 1**). Higher response amplitudes during pursuit were observed consistently in all models that allowed differences in that parameter (none, W, D, or W&D). This further supports that pursuit and fixation differed in respect to the response amplitude. For the natural temporal frequency, the difference is not as consistent. For subject A.C.S., the temporal frequency was lower during pursuit for two models (none and D) and higher for two other models (A and A&D). For subject HO, the temporal frequency was lower during pursuit for three models (none, A, and D) and higher only for one model (A&D). Please note that especially the models with a higher temporal frequency during pursuit showed a very low relative probability of AIC and BIC. Hence, if there were any changes in the temporal frequency of the TIRF, it was lowered during pursuit. The damping ratio was lower during pursuit or identical except for one case (subject HO and model W).

Fig. 4 shows the measured contrast sensitivity, the fits for the best model (W&D), and the resulting TIRF. For both subjects, the TIRF is nearly monophasic, which would result in a low-pass shape of the TCSF. This is in line with previous reports of the low-pass characteristics of the chromatic TCSF (Kelly, 1975, 1983). The monophasic character of the TIRF holds true for all fitted models indicated by the large damping values.

Discussion

In Experiment 1, we measured chromatic contrast sensitivity for two-pulse stimuli with different SOAs. We showed that the sensitivity improvement by smooth pursuit occurred for all SOA conditions. Furthermore, we fitted TIRF to the data and compared several models that allowed differences between fixation and smooth pursuit on different model dimensions. We could show that a model with equal natural temporal frequency and equal damping ratio during fixation and pursuit fitted the data better than any other model. Hence, the chromatic TIRF seemed not to be shifted along the time axis during smooth pursuit and fixation. Instead, the major difference between smooth pursuit and fixation could be expressed as a multiplicative scaling of chromatic sensitivity. As we previously showed that the sensitivity enhancement is not accomplished by an increased spatial integration (Schütz et al., 2008), it is most likely that the sensitivity enhancement is accomplished by an increased contrast gain. This is a physiologically plausible hypothesis as it has been shown that the contrast gain can be increased by feedback connections: cooling of V1 and thereby reducing feedback to LGN reduces the contrast gain in both magnocellular and parvocellular neurons (Przybyszewski et al., 2000). Attention is another example of a feedback-based neuronal modulation, which can occur as early as in the LGN (O'Connor et al., 2002; McAlonan et al., 2008).

Recently, it has been reported that the visual system integrates color along a motion trajectory, which can lead to color mixing (Nishida et al., 2007) or to an increase of chromatic flicker fusion frequency (Watanabe & Nishida, 2007). This mechanism probably helps to reduce motion blur (Burr, 1980). Furthermore, it has been shown that the execution of smooth pursuit additionally increases the flicker fusion frequency (Terao et al., 2008). Previous results (Schütz et al., 2008) and the results of this experiment suggest that the temporal resolution is increased by an increased contrast gain at all temporal frequencies and not by a speeding up of the TIRF.

Several studies investigated the effects of smooth pursuit on luminance processing. It has been shown that the natural temporal frequency is higher during pursuit than during fixation (Bedell et al., 2003; Tong et al., 2006). Interestingly, the natural temporal frequency seems to be even higher for motion against pursuit direction. In a previous study, we measured temporal contrast sensitivity for luminance stimuli (Schütz et al., 2007). Although the major finding was an overall reduction of sensitivity during smooth

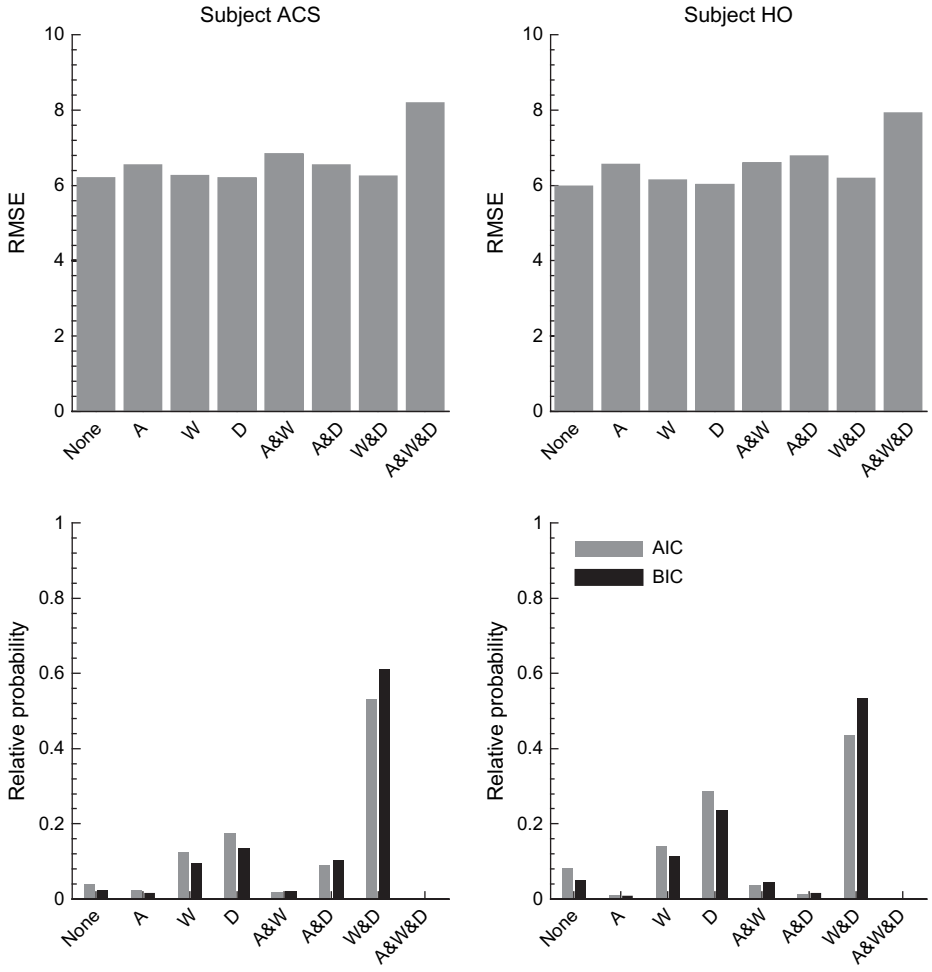

Fig. 2. Experiment 1: Quality of model fit. The two columns show the data for two subjects. The upper row shows the RMSE for the seven different models. The lower row shows the relative probability of the AIC in gray and the BIC (Schwarz, 1978) in black for the different models. Superior models are indicated by a lower RMSE and higher relative probability. Each model name contains the parameters that are fixed to equal values during fixation and pursuit.

pursuit and an additional reduction for motion opposite to pursuit, there was also a nonsignificant trend for a shift to higher temporal frequencies during pursuit. Another effect, which might be related to the temporal changes of luminance processing, is the selectively reduced extent of perceived motion smear during smooth pursuit for motion in the opposite direction (Bedell & Lott, 1996; Tong et al., 2005, 2007). As such, a suppression of motion smear also occurs during passive eye movements, and it has been concluded that the effect is at least partially caused by proprioceptive signals (Tong et al., 2008). Interestingly, such a proprioceptive feedback signal has been found recently in the somatosensory cortex (Wang et al., 2007).

During saccadic eye movements, sensitivity for low–spatial frequency luminance stimuli is suppressed, whereas sensitivity for color and high–spatial frequency luminance stimuli is unaffected (Ross et al., 1996, 2001). This suppression scales with the amplitude of saccades (Mitrani et al., 1970; Stevenson et al., 1986; Ridder & Tomlinson, 1997) and is triggered by an extraretinal signal (Diamond et al., 2000) and has been associated with a selective suppression of the magnocellular pathway (Burr et al., 1994; Uchikawa & Sato, 1995). The suppression is further accompanied by an acceleration of the TIRF for luminance stimuli but not for chromatic stimuli (Burr & Morrone, 1996). Burr and Morrone 1996 explained the speeding up of the TIRF by a reduced contrast gain in magnocellular neurons. It has been shown that a reduction of contrast gain is strongest at low temporal frequencies for magnocellular neurons (Benardete et al., 1992), which might result in a speeding up of the TIRF. Consistent with that explanation, the impulse response of magnocellular neurons speeds up during saccades, albeit the response magnitude was only weakly suppressed (Reppas et al., 2002).

Experiment 2: Spatial contrast sensitivity function for luminance

As noted above, there are several reports that luminance processing is affected by smooth pursuit eye movements. Bedell et al. showed that the extent of perceived motion smear is reduced during smooth pursuit for all motion with a directional component opposite to pursuit (Bedell & Lott, 1996; Tong et al., 2005, 2007). They also reported that the TIRF is speeded up during smooth pursuit (Bedell et al., 2003) and that this effect is stronger for stimuli moving against the pursuit direction (Tong et al., 2006). In line with these asymmetries, we found a reduction of temporal contrast sensitivity for motion against pursuit (Schütz et al., 2007).

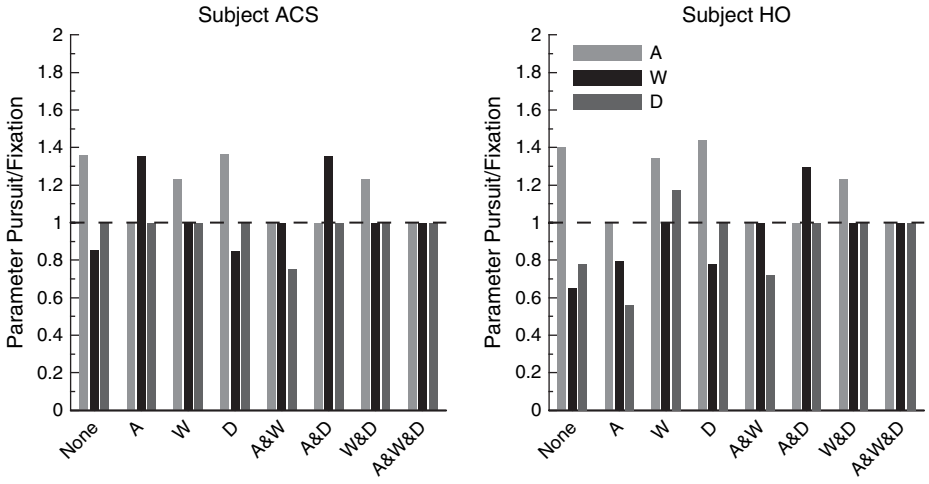

Fig. 3. Experiment 1: Parameters ratios between fixation and pursuit. The two columns show the data for two subjects. The light gray bars indicate parameter A, the black bars indicate parameter W, and the medium gray bars indicate parameter D. The dashed horizontal line indicates points where parameters are equal during smooth pursuit and fixation.

Moreover, we found a slight suppression of luminance sensitivity in the periphery for 1 cpd Gabor stimuli (Schütz et al., 2007) and for a line stimulus, consisting of low spatial frequencies (Schütz et al., 2008). Interestingly, sensitivity can also be improved by smooth pursuit not only for color stimuli but also for high–spatial frequency luminance stimuli (Schütz et al., 2008). In all these experiments, luminance sensitivity was only measured at single spatial frequencies. To get a more complete picture about the sensitivity changes during smooth pursuit, we measured the spatial contrast sensitivity function (SCSF) for luminance over a wide range of spatial frequencies. We did not measure the SCSF for color because color sensitivity is strongly affected by chromatic aberration at medium and high spatial frequencies (Flitcroft, 1989; Marimont & Wandell, 1994).

Materials and methods

If not otherwise stated, methods are the same as in Experiment 1.

Design

We estimated the SCSF for two different types of stimuli: Gabors with a fixed aperture size (FSG) and Gabors with a fixed number of sinusoid cycles (FCG). Both types are standard psychophysical stimuli, included in the ModelFest data set (Watson & Ahumada, 2005). For the FSG, we measured contrast sensitivity for 12 spatial frequencies: 0.2, 0.3, 0.5, 0.7, 1.0, 1.5, 2.0, 3.0, 4.0, 5.0, 6.0, and 7.0 cpd. For the FCG, we measured contrast sensitivity for eight spatial frequencies: 0.7, 1.0, 1.5, 2.0, 3.0, 4.0, 5.0, and 6.0 cpd. Like in Experiment 1, we compared sensitivity during fixation and smooth pursuit. Subjects performed the experiment in several sessions. In each session, sensitivity for one spatial frequency and one Gabor type was measured interleaved during fixation and pursuit.

Subjects

One of the authors (A.C.S.) completed the experiment for both the FSG and the FCG. The naïve subject from Experiment 1 (HO) participated in the FSG experimental condition, and one new naïve subject (AE) participated in the FCG experimental condition. The new naïve subject was a female student of the Justus-Liebig University who was paid for her participation.

Visual stimuli

We used Gabor patches as detection targets. For the FSG, the Gaussian S.D. was set to 1 deg. For the FCG, the Gaussian S.D. was set to 4/spatial frequency. Hence, both types of stimuli were identical for a spatial frequency of 4 cpd. The phase of the Gabor was randomized in each trial. In general, it was not possible to create patches with spatial frequencies above 7 cpd because too few pixels would have been available to create a sinusoidal modulation, so that the pattern would have approximated a square wave pattern. With the FSG, it was also not possible to test spatial frequencies below 0.2 because otherwise only a very small part of one sinusoid cycle would have been present within the aperture. With the FCG Gabor, it was not possible to test spatial frequencies below 0.7 cpd due to limitations of our setup. To avoid any retinal image motion of the stimulus, we aligned the sinusoid of the Gabor horizontally and flashed the Gabor for one refresh cycle of the monitor.

Experimental procedure

We used a 2IFC procedure to measure contrast thresholds. We used the same bull's-eye as fixation respective pursuit target as in Experiment 1. Each interval followed the same eye movement protocol as in Experiment 1. Hence, a fixation interval lasted 1500 ms, and the Gabor was presented after 1000 ms. A pursuit interval lasted 2000 ms, and the Gabor was presented 1500 ms after interval onset when the pursuit target reached the screen center. The two intervals were always exactly the same except that a Gabor was presented only in one interval. Each interval had to be started *via* button press of the subject, which activated the drift correction of the eye tracker. As we wanted to measure foveal sensitivity, we presented the Gabor patches at the screen center superimposed by the pursuit respective fixation target. After two intervals, subjects had to indicate which interval contained a Gabor patch.

Psychophysical data analysis

We estimated contrast thresholds like in Experiment 1. To fit the SCSF, we used nine different functions that have been used previously (Watson & Ahumada, 2005). We used again the relative probabilities of the AIC and BIC to determine which function fits the data best (eqn. 4).

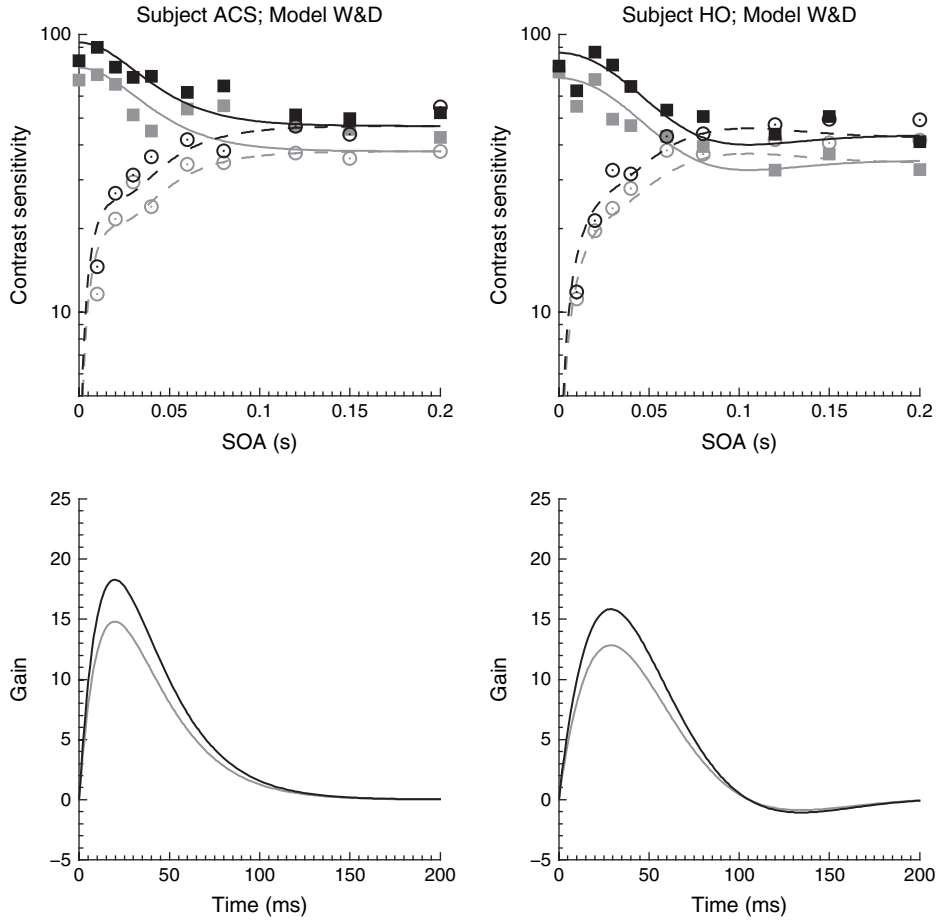

Fig. 4. Experiment 1: Color contrast sensitivity and the fitted model. The two columns show the data for two subjects. The upper row shows the measured contrast sensitivity and the model fit during pursuit (black) and fixation (gray) for in-phase stimulation (filled squares and continuous line) and out-of-phase stimulation (open circles and dashed line). The lower row shows the impulse response functions on which the model is based. For both subjects, model W&D has been used to fit the data.

Results

In this experiment, we measured luminance sensitivity for Gabor stimuli flashed at the fovea. In the first step, we fitted different contrast sensitivity functions to our data (Watson & Ahumada, 2005). In the FSG condition, all functions but HPmG could fit the data reasonably well, as indicated by RMSEs below 2. In the FCG condition, DoG, HmG, and HmH showed larger errors than the other functions. We used again the relative probability of the AIC and BIC to select the best fitting function (**Supplemental Figures 1 and 2; Supplemental Tables 2 and 3**) to account for the different number of free parameters of the functions. For subject A.C.S., function MS had the highest relative probability in the FSG condition (AIC: 0.34; BIC: 0.30) and in the FCG condition (AIC and BIC: 0.61). For subject HO, function HmH fitted the data best in terms of the relative probability of AIC (0.30) and BIC (0.27). Function LP fitted the data best for subject AE (AIC and BIC: 0.84). All the superior functions had four free parameters.

As can be seen from Fig. 5, there was a strong difference between the FSG and the FCG conditions. Whereas the FSG function shows a bandpass characteristic, the FCG data follow a low-pass characteristic. The low-pass shape of the FCG is consistent with previous reports of SCSF for brief flashes (Kelly, 1977). The attenuation at low spatial frequencies in the FSG function is probably caused by the reduced number of visible cycles of the sinusoid (Hoekstra et al., 1974; Savoy & McCann, 1975; Howell, 1978). Despite these large differences between the Gabor types, the pursuit-induced sensitivity modulations were quite similar for both types of Gabors, as can be seen from Fig. 6.

Next, we looked at the sensitivity differences between pursuit and fixation (Fig. 6). For subject A.C.S., sensitivity was higher during smooth pursuit for spatial frequencies above 3 cpd for both the FSG and the FCG conditions. Below 3 cpd, sensitivity was lower during pursuit and also consistent in both conditions. However, sensitivities were equal for spatial frequencies below 0.5 cpd in the FSG condition and below 1 cpd in the FCG condition. For subject HO, in the FSG condition, the picture was similar except that sensitivity during pursuit was higher than during fixation for spatial frequencies below 0.5 cpd. Subject AE, in the FCG condition, showed a higher sensitivity during pursuit for spatial frequencies above 2 cpd and a lower sensitivity for spatial frequencies below 2 cpd. The maximal increase of sensitivity during pursuit was observable at the highest measured spatial frequency of 7 cpd for all subjects. The maximum decrease of sensitivity was measured at 1.5 cpd for subject A.C.S. in the FSG condition and at 2 cpd in the FCG condition. For subject HO, the peak decrease occurred at 0.7 cpd and for subject AE at 1.5 cpd.

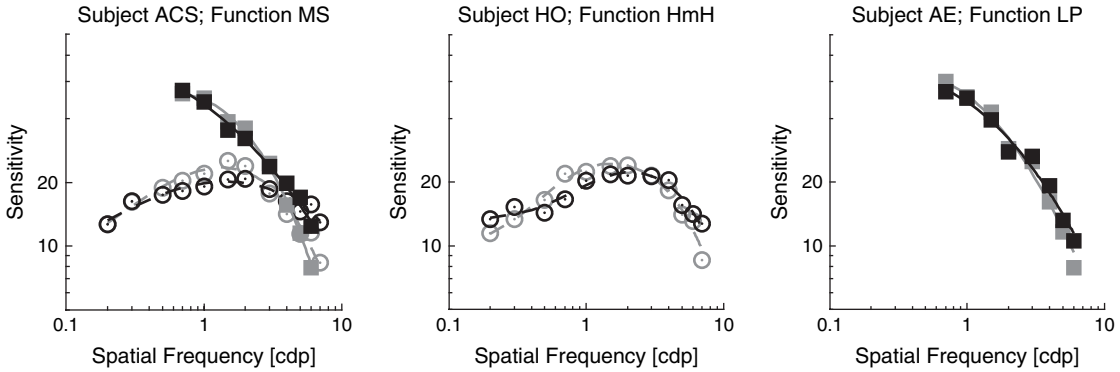

Fig. 5. Experiment 2: Luminance contrast sensitivity and the fitted functions. The three columns show the data for three subjects. Data for fixation are plotted in gray; data for pursuit are plotted in black. Open circles and dashed lines show data for FSG; filled squares and continuous lines show data for FCG. Markers denote measured sensitivities; the lines represent the fitted function MS for subject A.C.S., function HmH for subject HO, and function LP for subject AE.

Discussion

We measured the SCSF for luminance during pursuit and fixation. During pursuit, contrast sensitivity was consistently improved for spatial frequencies above 3 cpd and reduced for intermediate spatial frequencies for all subjects and for both the FSG and the FCG conditions. For low spatial frequencies, there was no consistent pattern across subjects and conditions. For subject A.C.S., there was no sensitivity difference between fixation and pursuit for low spatial frequencies. Subject HO, in the FSG condition, showed a higher sensitivity during pursuit at low spatial frequencies, whereas subject AE showed in the FCG condition a lower sensitivity during pursuit at low spatial frequencies. Hence, there seems to be no clear-cut influence of smooth pursuit on low spatial frequencies.

Previously, we found a suppression of luminance sensitivity for low spatial frequencies only in the periphery but not in the fovea (Schütz et al., 2007, 2008). In these previous experiments, we used a horizontal line that was modulated vertically by a Gaussian distribution with an s.d. of 0.5 deg. In the frequency domain, this stimulus is a Gaussian with an s.d. of 1.06 cpd. Hence, most of the energy of this stimulus was in a frequency range for which we did not find a clear suppression in the current study. Therefore, the previous finding that low–spatial frequency luminance sensitivity in the fovea is not suppressed during pursuit is consistent with the findings of the present experiment. Several factors might explain why the same stimulus presented in the periphery is slightly suppressed during pursuit: (i) retinal inhomogeneities, (ii) surround suppression in the periphery, and (iii) spatial attention shifts. One of the most important properties of the human visual system is inhomogeneity across the visual field. It is known that the sampling density of photoreceptors and retinal ganglion cells drops with distance to the fovea. This influences the limits of visual acuity (Merigan & Katz, 1990) and the SCSF (Kelly, 1984), which shifts to lower spatial frequencies at the periphery. It might be possible that the cutoff frequency for suppression *versus* enhancement during pursuit also changes across the retina. Foveal and peripheral processing also differs in respect to surround suppression effects. These effects are strongest for magnocellular neurons (Solomon et al., 2002) and are much weaker at the fovea (Xing & Heeger, 2000). Although we used uniform gray backgrounds in our experiments, the screen border moved on the retina during smooth pursuit, which might suppress peripheral luminance sensitivity. Another qualitative difference between foveal and peripheral processing is related to spatial attention. The premotor theory of attention (Rizzolatti et al., 1987) assumes that there is an obligatory link between covert and overt attention shifts. In that way, attention should be bounded to the foveal pursuit target during the execution of smooth pursuit. Indeed, several studies reported interference between pursuit and spatial attention shifts for steady-state pursuit (Khurana & Kowler, 1987; Hutton & Tegally, 2005; Kerzel & Ziegler, 2005; Kerzel

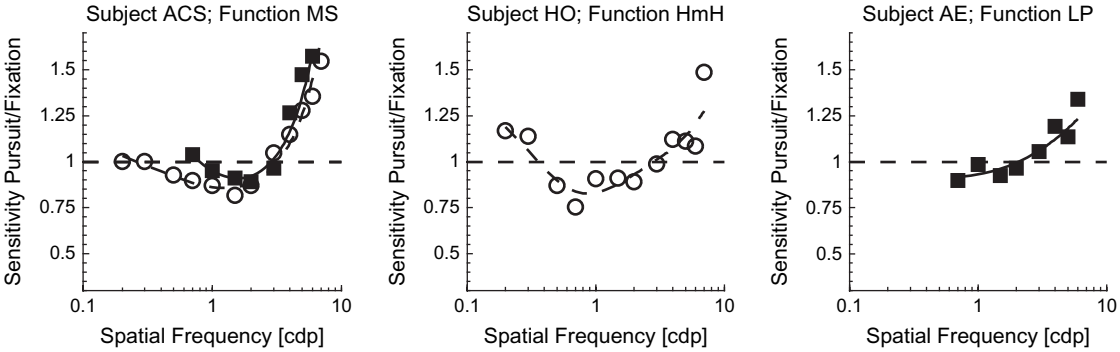

Fig. 6. Experiment 2: Luminance sensitivity ratio between fixation and pursuit. The three columns show the data for three subjects. Open circles and dashed lines show data for FSG; filled squares and continuous lines show data for FCG. Markers represent measured sensitivity ratios. The lines represent the fitted sensitivity ratio based on the function MS for subject A.C.S., function HmH for subject HO, and function LP for subject AE. The dashed horizontal line indicates points with equal sensitivity during fixation and pursuit.

et al., 2008). Hence, the binding of spatial attention to the pursuit target might reduce peripheral contrast sensitivity.

There is good evidence that the TIRF for luminance is speeded up during smooth pursuit (Bedell et al., 2003; Tong et al., 2006). One may ask if the observed changes of the SCSF are related to the faster temporal impulse response during smooth pursuit. As spatial and temporal contrast sensitivities are only separable for high temporal or spatial frequencies (Koenderink & Doorn, 1979), one has to assume that any change in spatial contrast sensitivity affects temporal contrast sensitivity and vice versa. To disentangle these two factors, one would have to measure the whole 2D spatio-temporal surface during fixation and pursuit.

It is known that the human SCSF is the envelope of multiple spatial frequency channels (Campbell & Robson, 1968; De Valois & De Valois, 1988). Independent spatial frequency channels have been observed even for second-order stimuli (Landy & Oruc, 2002). An open question is still how the SCSF for luminance reflects the sensitivity of the parvo- and magnocellular pathways. Several studies tried to identify at which spatial frequencies one pathway dominates the other. These studies used different methods and ended up with different estimations of the transition. By comparing contrast sensitivity for flicker and pattern detection, the transition between sustained and transient channels has been inferred between 3 and 5 cpd (King-Smith & Kulikowski, 1975). Legge (1978) observed quantitative differences of pattern masking below and above 1.5 cpd and interpreted this also in terms of sustained and transient channels. A similar transition between 1 and 2 cpd was obtained by Burbeck and Kelly (1981). Using a discrimination task in pulsed- and steady-pedestal paradigms, a transition between inferred parvo- and magnocellular pathways has been determined at 4 cpd (Leonova et al., 2003). Besides psychophysical measurements, attempts have been made to associate magno- and parvocellular activity with differential electroencephalography (EEG) activity (Baseler & Sutter, 1997; Arakawa et al., 1999; Ellemberg et al., 2001). Measurements of the contrast dependency of visual evoked potentials at different spatial frequencies suggest that the magno- and parvo parvocellular pathways both contribute at intermediate spatial frequencies (Ellemberg et al., 2001).

Physiological studies showed that parvocellular lesions impair sensitivity for high spatial and low temporal frequencies (Merigan & Eskin, 1986; Merigan, 1989; Merigan et al., 1991), whereas magnocellular lesions cause mainly deficits for high temporal frequencies (Merigan & Maunsell, 1990; Merigan et al., 1991). However, single-cell recordings of magno- and parvocellular neurons showed that the spatial and temporal resolution of individual neurons can be much higher than the perceptual resolution (Derrington & Lennie, 1984).

To conclude, sensitivity at high spatial frequencies seems to depend on parvocellular activity and at low spatial frequencies on magnocellular activity, and both pathways are probably involved at medium spatial frequencies. Hence, our finding of an increased sensitivity during pursuit for spatial frequencies above 3 cpd would be compatible with increased parvocellular sensitivity during pursuit. The suppression at intermediate spatial frequencies might result from the noise introduced by an enhanced parvocellular activity, which is not optimal for these spatial frequencies.

General discussion

In two experiments, we investigated the temporal and spatial characteristics of the sensitivity enhancement observed during smooth pursuit. In Experiment 1, we showed that the chromatic TIRF differs between fixation and pursuit mostly in respect to the gain but hardly in respect to the natural temporal frequency. Thus, the sensitivity enhancement for color is present at all temporal frequencies. In Experiment 2, we showed that luminance sensitivity is enhanced for spatial frequencies above 2–3 cpd and suppressed for intermediate spatial frequencies between 0.5 and 3 cpd. Below 0.5 cpd, no consistent pattern was observed.

During saccades, sensitivity is selectively reduced for low–spatial frequency luminance stimuli (Burr et al., 1982, 1994). Depending on the illuminance level, spatial frequencies below 1.5 cpd or below 0.2 cpd are suppressed. Based on the psychophysical results, it has been concluded that saccadic suppression most probably takes place at the magnocellular neurons in the LGN (Burr et al., 1994). However, physiological studies found strong suppression of neural activity only in extrastriate areas MT and MST (Thiele et al., 2002; Ibbotson et al., 2007) and in superficial layers of the SC (Robinson & Wurtz, 1976), whereas suppression in LGN (Reppas et al., 2002; Royal et al., 2006) or V1 (Wurtz, 1969*a*,*b*) was not present or rather weak. Hence, it might be that the sensitivity loss during saccades does not take place in the retinogeniculate-cortical pathway but rather in the SC-pulvinar-cortical pathway (see Wurtz, 2008, for a review). This example shows that psychophysical results have to be interpreted cautiously in respect to the underlying neural mechanisms. However, if one assumes that the observed changes of chromatic sensitivity and luminance sensitivity for high spatial frequencies are mediated by the same neural structure, it is quite unlikely that the SC-pulvinar-cortical pathway is involved because neurons in the superficial layers of the SC do not receive inputs from color-opponent cells (Schiller & Malpeli, 1977; Schiller et al., 1979) and do not respond to isoluminant stimuli (Marrocco & Li, 1977). However recently color-related activity has been found for neurons in the intermediate layers of the SC (White et al., 2008).

If one assumes that the visual system actively changes neuronal properties to achieve the observed sensitivity changes, the aim of these changes is still unclear. Several properties and consequences of smooth pursuit might give the reasons for the sensitivity modulations: First, they might be related to the recognition of the tracked object. An increase of sensitivity for color and high spatial frequencies should facilitate the recognition of the tracked object. Second, the sensitivity modulations might aim at a facilitation of the perception of the stationary background. During smooth pursuit, all stationary objects move on the retina, which increases the temporal frequency of these objects and hampers perception by introducing motion blur (Burr, 1980). However, a clear perception of the stationary context is important during smooth pursuit because pursuit can be executed for a relatively long time. It is known that the TCSF has a low-pass shape for color and high–spatial frequency luminance patterns (if the pattern is presented for longer durations). Hence, the sensitivity for these types of stimuli would suffer in particular from the retinal motion. The reported sensitivity enhancement might counteract these detrimental effects of retinal motion. This view is supported by the finding that chromatic sensitivity is also enhanced during optokinetic nystagmus (OKN) but not during visually enhanced active vestibulo-ocular reflex (Schütz et al., 2009). Although both types of eye movements can result in the same eye-in-head motion as pursuit, only OKN causes a similar retinal motion. Third, the sensitivity modulations might reflect a modification of motion processing to the needs during pursuit. Smooth pursuit essentially stabilizes the tracked object on the retina so that only small residual retinal velocities are present. To improve the tracking performance, it

might be beneficial to increase sensitivity for small velocities. Psychophysical and physiological evidence suggests that there are at least two motion mechanisms: one mechanism that encodes primarily color contrasts and slow velocities and another mechanism that encodes primarily luminance contrasts and fast velocities (Gegenfurtner & Hawken, 1995, 1996). It is known that the perceived speed is underestimated for isoluminant colored targets (Cavanagh et al., 1984). Interestingly, we found that this underestimation happens only during fixation but not during steady-state pursuit (Braun et al., 2008). In this view, the improved sensitivity for color and fine spatial details would be a side effect of a stronger weighting of the slow color motion mechanism during smooth pursuit.

Acknowledgments

This work was supported by the DFG Forschergruppe FOR 560 "Perception and Action." We thank Harold Bedell for helpful discussion, Kurt Debono for help with improving the English, Elisabeth Baumgartner for help with data collection, and subjects HO and AE for participation in the lengthy experiments.

References

Akaike, H. (1974). A new look at the statistical model identification. *IEE Transactions on Automatic Control AC* **19**, 716–723.

Arakawa, K., Tobimatsu, S., Tomoda, H., Kira, J. & Kato, M. (1999). The effect of spatial frequency on chromatic and achromatic steady-state visual evoked potentials. *Clinical Neurophysiology* **110**, 1959–1964.

Barlow, H.B. (1958). Temporal and spatial summation in human vision at different background intensities. *The Journal of Physiology* **141**, 337–350.

Baseler, H.A. & Sutter, E.E. (1997). M and P components of the VEP and their visual field distribution. *Vision Research* **37**, 675–690.

Bedell, H.E. & Lott, L.A. (1996). Suppression of motion-produced smear during smooth pursuit eye movements. *Current Biology* **6**, 1032–1034.

Bedell, H.E., Ramamurthy, M., Patel, S.S. & Vu-Yu, L.P. (2003). The temporal impulse response function during smooth pursuit. *Journal of Vision* **3**, 210a.

Bedell, H.E., Ramamurthy, M., Patel, S.S., Subramaniam, S., Vu-Yu, L.P. & Tong, J. (2008). The temporal impulse response function in infantile nystagmus. *Vision Research* **48**, 1575–1583.

Benardete, E.A. & Kaplan, E. (1999). The dynamics of primate M retinal ganglion cells. *Visual Neuroscience* **16**, 355–368.

Benardete, E.A., Kaplan, E. & Knight, B.W. (1992). Contrast gain control in the primate retina: P cells are not X-like, some M cells are. *Visual Neuroscience* **8**, 483–486.

Braun, D.I., Mennie, N., Rasche, C., Schutz, A.C., Hawken, M.J. & Gegenfurtner, K.R. (2008). Smooth pursuit eye movements to isoluminant targets. *Journal of Neurophysiology* **100**, 1287–1300.

Burbeck, C.A. & Kelly, D.H. (1981). Contrast gain measurements and the transient/sustained. *Journal of the Optical Society of America* **71**, 1335–1342.

Burnham, K.P. & Anderson, D.R. (2002). *Model Selection and Multimodel Inference: A Practical Information-Theoretic Approach*. New York: Springer.

Burr, D.C. (1980). Motion smear. *Nature* **284**, 164–165.

Burr, D.C., Holt, J., Johnstone, J.R. & Ross, J. (1982). Selective depression of motion sensitivity during saccades. *The Journal of Physiology* **333**, 1–15.

Burr, D.C. & Morrone, M.C. (1993). Impulse-response functions for chromatic and achromatic stimuli. *Journal of the Optical Society of America A* **10**, 1706–1713.

Burr, D.C. & Morrone, M.C. (1996). Temporal impulse response functions for luminance and colour during saccades. *Vision Research* **36**, 2069–2078.

Burr, D.C., Morrone, M.C. & Ross, J. (1994). Selective suppression of the magnocellular visual pathway during saccadic eye movements. *Nature* **371**, 511–513.

Campbell, F.W. & Robson, J.G. (1968). Application of Fourier analysis to the visibility of gratings. *The Journal of Physiology* **197**, 551–566.

Cavanagh, P., Tyler, C.W. & Favreau, O.E. (1984). Perceived velocity of moving chromatic gratings. *Journal of the Optical Society of America A* **1**, 893–899.

Derrington, A.M., Krauskopf, J. & Lennie, P. (1984). Chromatic mechanisms in lateral geniculate nucleus of macaque. *The Journal of Physiology* **357**, 241–265.

Derrington, A.M. & Lennie, P. (1984). Spatial and temporal contrast sensitivities of neurones in lateral geniculate nucleus of macaque. *The Journal of Physiology* **357**, 219–240.

De Valois, R.L. & De Valois, K.K. (1988). *Spatial Vision*. New York: Oxford University Press.

Diamond, M.R., Ross, J. & Morrone, M.C. (2000). Extraretinal control of saccadic suppression. *Journal of Neuroscience* **20**, 3449–3455.

Ellemberg, D., Hammarrenger, B., Lepore, F., Roy, M.S. & Guillemot, J.P. (2001). Contrast dependency of VEPs as a function of spatial frequency: The parvocellular and magnocellular contributions to human VEPs. *Spatial Vision* **15**, 99–111.

Eskew, R.T. Jr., Stromeyer, C.F. III. & Kronauer, R.E. (1994). Temporal properties of the red-green chromatic mechanism. *Vision Research* **34**, 3127–3137.

Flitcroft, D.I. (1989). The interactions between chromatic aberration, defocus and stimulus chromaticity: Implications for visual physiology and colorimetry. *Vision Research* **29**, 349–360.

Gegenfurtner, K.R. & Hawken, M.J. (1995). Temporal and chromatic properties of motion mechanisms. *Vision Research* **35**, 1547–1563.

Gegenfurtner, K.R. & Hawken, M.J. (1996). Interaction of motion and color in the visual pathways. *Trends in Neurosciences* **19**, 394–401.

Hoekstra, J., van der Goot, D.P., van den Brink, G. & Bilsen, F.A. (1974). The influence of the number of cycles upon the visual contrast threshold for spatial sine wave patterns. *Vision Research* **14**, 365–368.

Holt, E.B. (1903). Eye movements and central anaesthesia. *Psychological Review* **4**, 3–45.

Howell, E.R. (1978). The functional area for summation to threshold for sinusoidal gratings. *Vision Research* **18**, 369–374.

Hutton, S.B. & Tegally, D. (2005). The effects of dividing attention on smooth pursuit eye tracking. *Experimental Brain Research* **163**, 306–313.

Ibbotson, M.R., Price, N.S., Crowder, N.A., Ono, S. & Mustari, M.J. (2007). Enhanced motion sensitivity follows saccadic suppression in the superior temporal sulcus of the macaque cortex. *Cerebral Cortex* **17**, 1129–1138.

Ikeda, M. (1965). Temporal summation of positive and negative flashes in the visual system. *Journal of the Optical Society of America* **55**, 1527–1534.

Kelly, D.H. (1975). Luminous and chromatic flickering patterns have opposite effects. *Science* **188**, 371–372.

Kelly, D.H. (1977). Visual contrast sensitivity. *Optica Acta* **24**, 107–129.

Kelly, D.H. (1983). Spatiotemporal variation of chromatic and achromatic contrast thresholds. *Journal of the Optical Society of America* **73**, 742–750.

Kelly, D.H. (1984). Retinal inhomogeneity. I. Spatiotemporal contrast sensitivity. *Journal of the Optical Society of America A* **1**, 107–113.

Kerzel, D., Souto, D. & Ziegler, N.E. (2008). Effects of attention shifts to stationary objects during steady-state smooth pursuit eye movements. *Vision Research* **48**, 958–969.

Kerzel, D. & Ziegler, N.E. (2005). Visual short-term memory during smooth pursuit eye movements. *Journal of Experimental Psychology: Human Perception and Performance* **31**, 354–372.

Khurana, B. & Kowler, E. (1987). Shared attentional control of smooth eye movement and perception. *Vision Research* **27**, 1603–1618.

King-Smith, P.E. & Kulikowski, J.J. (1975). Pattern and flicker detection analysed by subthreshold summation. *The Journal of Physiology* **249**, 519–548.

Koenderink, J.J. & Doorn, A.J.v. (1979). Spatiotemporal contrast detection threshold surface is bimodal. *Optics Letters* **4**, 32–34.

Landy, M.S. & Oruc, I. (2002). Properties of second-order spatial frequency channels. *Vision Research* **42**, 2311–2329.

Lee, B.B., Pokorny, J., Smith, V.C. & Kremers, J. (1994). Responses to pulses and sinusoids in macaque ganglion cells. *Vision Research* **34**, 3081–3096.

Legge, G.E. (1978). Sustained and transient mechanisms in human vision: Temporal and spatial properties. *Vision Research* **18**, 69–81.

Leonova, A., Pokorny, J. & Smith, V.C. (2003). Spatial frequency processing in inferred PC- and MC-pathways. *Vision Research* **43**, 2133–2139.

Levitt, H. (1971). Transformed up-down methods in psychoacoustics. *Journal of the Acoustical Society of America* **49**, 467–477.

Marimont, D.H. & Wandell, B.A. (1994). Matching color images: The effects of axial chromatic aberration. *Journal of the Optical Society of America A* **11**, 3113–3122.

Marrocco, R.T. & Li, R.H. (1977). Monkey superior colliculus: Properties of single cells and their afferent inputs. *Journal of Neurophysiology* **40**, 844–860.

McAlonan, K., Cavanaugh, J. & Wurtz, R.H. (2008). Guarding the gateway to cortex with attention in visual thalamus. *Nature* **456**, 391–394.

Merigan, W.H. (1989). Chromatic and achromatic vision of macaques: Role of the P pathway. *Journal of Neuroscience* **9**, 776–783.

Merigan, W.H. & Eskin, T.A. (1986). Spatio-temporal vision of macaques with severe loss of P beta retinal ganglion cells. *Vision Research* **26**, 1751–1761.

Merigan, W.H. & Katz, L.M. (1990). Spatial resolution across the macaque retina. *Vision Research* **30**, 985–991.

Merigan, W.H., Katz, L.M. & Maunsell, J.H. (1991). The effects of parvocellular lateral geniculate lesions on the acuity and contrast sensitivity of macaque monkeys. *Journal of Neuroscience* **11**, 994–1001.

Merigan, W.H. & Maunsell, J.H. (1990). Macaque vision after magnocellular lateral geniculate lesions. *Visual Neuroscience* **5**, 347–352.

Mitrani, L., Yakimoff, N. & Mateeff, S. (1970). Dependence of visual suppression on the angular size of voluntary saccadic eye movements. *Vision Research* **10**, 411–415.

Nishida, S., Watanabe, J., Kuriki, I. & Tokimoto, T. (2007). Human visual system integrates color signals along a motion trajectory. *Current Biology* **17**, 366–372.

O'Connor, D.H., Fukui, M.M., Pinsk, M.A. & Kastner, S. (2002). Attention modulates responses in the human lateral geniculate nucleus. *Nature Neuroscience* **5**, 1203–1209.

Olzak, L.A. & Thomas, J.P. (1986). Seeing spatial patterns. In *Handbook of Perception and Human Performance*, **Vol. 7**, ed. Boff, K.R., Kaufman, L. & Thomas, J.P., pp. 1–56. New York: Wiley.

Przybyszewski, A.W., Gaska, J.P., Foote, W. & Pollen, D.A. (2000). Striate cortex increases contrast gain of macaque LGN neurons. *Visual Neuroscience* **17**, 485–494.

Rashbass, C. (1970). The visibility of transient changes of luminance. *The Journal of Physiology* **210**, 165–186.

Reppas, J.B., Usrey, W.M. & Reid, R.C. (2002). Saccadic eye movements modulate visual responses in the lateral geniculate nucleus. *Neuron* **35**, 961–974.

Ridder, W.H. III. & Tomlinson, A. (1997). A comparison of saccadic and blink suppression in normal observers. *Vision Research* **37**, 3171–3179.

Rizzolatti, G., Riggio, L., Dascola, I. & Umilta, C. (1987). Reorienting attention across the horizontal and vertical meridians: Evidence in favor of a premotor theory of attention. *Neuropsychologia* **25**, 31–40.

Robinson, D.L. & Wurtz, R.H. (1976). Use of an extraretinal signal by monkey superior colliculus neurons to distinguish real from self-induced stimulus movement. *Journal of Neurophysiology* **39**, 852–870.

Ross, J., Burr, D. & Morrone, C. (1996). Suppression of the magnocellular pathway during saccades. *Behavioral Brain Research* **80**, 1–8.

Ross, J., Morrone, M.C., Goldberg, M.E. & Burr, D.C. (2001). Changes in visual perception at the time of saccades. *Trends in Neurosciences* **24**, 113–121.

Royal, D.W., Sary, G., Schall, J.D. & Casagrande, V.A. (2006). Correlates of motor planning and postsaccadic fixation in the macaque monkey lateral geniculate nucleus. *Experimental Brain Research* **168**, 62–75.

Savoy, R.L. & McCann, J.J. (1975). Visibility of low-spatial-frequency sine-wave targets: Dependence on number of cycles. *Journal of the Optical Society of America* **65**, 343–350.

Schiller, P.H. & Malpeli, J.G. (1977). Properties and tectal projections of monkey retinal ganglion cells. *Journal of Neurophysiology* **40**, 428–445.

Schiller, P.H., Malpeli, J.G. & Schein, S.J. (1979). Composition of geniculostriate input ot superior colliculus of the rhesus monkey. *Journal of Neurophysiology* **42**, 1124–1133.

Schütz, A.C., Braun, D.I. & Gegenfurtner, K.R. (2009). Chromatic contrast sensitivity during optokinetic nystagmus, visually-enhanced vestibulo-ocular reflex and smooth pursuit eye movements. *Journal of Neurophysiology* **101**, 2317–2327.

Schütz, A.C., Braun, D.I., Kerzel, D. & Gegenfurtner, K.R. (2008). Improved visual sensitivity during smooth pursuit eye movements. *Nature Neuroscience* **11**, 1211–1216.

Schütz, A.C., Delipetkos, E., Braun, D.I., Kerzel, D. & Gegenfurtner, K.R. (2007). Temporal contrast sensitivity during smooth pursuit eye movements. *Journal of Vision* **7**, 1–15.

Schwarz, G. (1978). Estimating the dimension of a model. *The Annals of Statistics* **6**, 461–464.

Solomon, S.G., White, A.J. & Martin, P.R. (2002). Extraclassical receptive field properties of parvocellular, magnocellular, and koniocellular cells in the primate lateral geniculate nucleus. *Journal of Neuroscience* **22**, 338–349.

Sperry, R.W. (1950). Neural basis of the spontaneous optokinetic response produced by visual inversion. *Journal of Comparative and Physiological Psychology* **43**, 482–489.

Stevenson, S.B., Volkmann, F.C., Kelly, J.P. & Riggs, L.A. (1986). Dependence of visual suppression on the amplitudes of saccades and blinks. *Vision Research* **26**, 1815–1824.

Terao, M., Watanabe, J., Yagi, A. & Nishida, S. (2008). Improvement of chromatic temporal resolution during smooth pursuit eye movement. *Journal of Vision* **8**, 663a.

Thiele, A., Henning, P., Kubischik, M. & Hoffmann, K.P. (2002). Neural mechanisms of saccadic suppression. *Science* **295**, 2460–2462.

Tong, J., Aydin, M. & Bedell, H.E. (2007). Direction and extent of perceived motion smear during pursuit eye movement. *Vision Research* **47**, 1011–1019.

Tong, J., Patel, S.S. & Bedell, H.E. (2005). Asymmetry of perceived motion smear during head and eye movements: Evidence for a dichotomous neural categorization of retinal image motion. *Vision Research* **45**, 1519–1524.

Tong, J., Patel, S.S. & Bedell, H.E. (2006). Asymmetrical modulation of the temporal impulse response during smooth pursuit. *Journal of Vision* **6**, 866a.

Tong, J., Stevenson, S.B. & Bedell, H.E. (2008). Signals of eye-muscle proprioception modulate perceived motion smear. *Journal of Vision* **8**, 1–6.

Uchikawa, K. & Ikeda, M. (1986). Temporal integration of chromatic double pulses for detection of equal-luminance wavelength changes. *Journal of the Optical Society of America A* **3**, 2109–2115.

Uchikawa, K. & Sato, M. (1995). Saccadic suppression of achromatic and chromatic responses measured by increment-threshold spectral sensitivity. *Journal of the Optical Society of America A* **12**, 661–666.

von Holst, E. & Mittelstaedt, H. (1950). Das Reafferenzprinzip. *Die Naturwissenschaften* **37**, 464–476.

Wang, X., Zhang, M., Cohen, I.S. & Goldberg, M.E. (2007). The proprioceptive representation of eye position in monkey primary somatosensory cortex. *Nature Neuroscience* **10**, 640–646.

Watanabe, J. & Nishida, S. (2007). Veridical perception of moving colors by trajectory integration of input signals. *Journal of Vision* **7**, 1–16.

Watson, A.B. (1979). Probability summation over time. *Vision Research* **19**, 515–522.

Watson, A.B. (1986). Temporal sensitivity. In *Handbook of Perception and Human Performance*, **Vol. 6**, ed. Boff, K.R., Kaufman, L. & Thomas, J.P., pp. 1–43. New York: Wiley.

Watson, A.B. & Ahumada, A.J. Jr. (2005). A standard model for foveal detection of spatial contrast. *Journal of Vision* **5**, 717–740.

White, B.J., Boehnke, S.E., Marino, R.A., Itti, L. & Munoz, D.P. (2008). Color Signals in the Primate Superior Colliculus. *Journal of Vision* **8**, 5a.

Wichmann, F.A. & Hill, N.J. (2001). The psychometric function: I. Fitting, sampling, and goodness of fit. *Perception & Psychophysics* **63**, 1293–1313.

Wurtz, R.H. (1969*a*). Comparison of effects of eye movements and stimulus movements on striate cortex neurons of the monkey. *Journal of Neurophysiology* **32**, 987–994.

Wurtz, R.H. (1969*b*). Response of striate cortex neurons to stimuli during rapid eye movements in the monkey. *Journal of Neurophysiology* **32**, 975–986.

Wurtz, R.H. (2008). Neuronal mechanisms of visual stability. *Vision Research* **48**, 2070–2089.

Wyatt, H.J. (1998). Detecting saccades with jerk. *Vision Research* **38**, 2147–2153.

Xing, J. & Heeger, D.J. (2000). Center-surround interactions in foveal and peripheral vision. *Vision Research* **40**, 3065–3072.

Supplemental Data

Supplemental materials can be viewed in this issue of VNS by visiting journals.cambridge.org

Supplemental Figure 1. Experiment 2, fixed-size Gabor: Quality of function fit. The two columns show the data for two subjects. The upper row shows the RMSE for the nine different functions. The lower row shows the relative probability of the AIC in gray and the BIC in black for the different functions. Superior functions are indicated by a lower RMSE and a higher relative probability.

Supplemental Figure 2. Experiment 2, fixed cycles Gabor: Quality of function fit. Conventions are the same as in Supplemental Figure 1.

Supplemental Table 1. Experiment 1: Overview of fitted models. Each model name contains the parameters that are fixed to equal values during fixation and pursuit. A, response gain; W, the natural temporal frequency; D, the damping ratio.

Supplemental Table 2. Experiment 2, fixed-size Gabor: Overview of fitted functions. A, response gain; f0, the high-frequency cutoff; f1, the low-frequency cutoff; b, the gain of the low-frequency attenuation; and p, the exponent.

Supplemental Table 3. Experiment 2, fixed cycles Gabor: Overview of fitted functions. Conventions are the same as in Supplemental Table 2.